Electrochemistry Communications 121 (2020) 106866

Contents lists available at ScienceDirect

Electrochemistry Communications

journal homepage: www.elsevier.com/locate/elecom

The common features of tetrameric ion channels and the role of electrostatic interactions

Rolando Guidelli

Department of Chemistry "Ugo Schiff", Florence University, Via della Lastruccia 3, 50019 Sesto Fiorentino (Firenze), Italy

ARTICLE INFO

Keywords:
Voltage-gated ion channels
Shaker potassium channel
Sodium channels
HVA calcium channels
T-type calcium channels

ABSTRACT

The three tetrameric voltage-gated K^+, Na^+, and Ca^{2+} ion channels share a high number of common structural features. Moreover, they share a common charge distribution over the corresponding molecular components. These common features point to an energetically favored pathway of channel opening. This pathway starts from an ion channel conformation consisting of the activation gate closed and the inactivation gate (i.e., the selectivity filter) open. As a consequence of a depolarizing pulse, the stepwise outward movement of the four S4 helices triggers a series of interlinked electrostatic attractive interactions leading to complete opening of the ion channels. The assumption of a stepwise outward movement of the S4 helices is supported not only by the possibility of accounting for the salient kinetic features of these ion channels with a minimum of two, or at most three, free parameters, but also by a similar experimental stepwise movement of the gating charge.

1. Introduction

Biological membranes are not permeable to inorganic ions; nonetheless, the movement of ions in and out of a cell is critical for their normal activity. Ions do not pass through the plasma membrane by simple diffusion; rather, their transport is mediated by protein-lined pores called ion channels. Ion transport through ion channels is an example of passive transport because these channels move a specific permeant cation from the membrane side, where its electrochemical potential is higher, to that where it is lower. Voltage-gated K^+, Na^+, and Ca^{2+} channels consist of four identical or homologous units and are referred to as tetrameric ion channels. Each unit is composed of six transmembrane α-helices (S1–S6). The four repeated units (I–IV) are circularly arranged around a central pore (CP). In K^+ channels the four units are not covalently linked together and are called *subunits*, while in Na^+ and Ca^{2+} channels they are connected by conformationally flexible loops and are called *domains*. In what follows, to simplify the notation, the term domain will also be used to denote the K^+ subunit (Fig. 1).

By voltage-gated Na^+ channel we mean its α subunit of 260 kDa, without its smaller β-subunit of 30–40 kDa [1]. Even though the β subunit is required for normal kinetics of gating, the sole α subunit is sufficient for functional expression of the Na^+ channel [2]. Ca^{2+} channels show two well distinct types, namely high voltage activated (HVA) Ca^{2+} channels and low voltage activated (LVA) ones [3]. The latter are also called T-type or Ca_v3 Ca^{2+} channels. LVA Ca^{2+} channels require smaller activating potential steps and inactivate faster, more completely and at more negative potentials than HVA Ca^{2+} channels [4]. The Ca^{2+} channel subunit with a structure quite similar to that of Shaker K^+ and Na^+ channels is the $\alpha 1$ subunit [5,6]. In HVA Ca^{2+} channels the single expressed $\alpha 1$ subunit is sufficient to produce Ca^{2+} currents, but with a low expression level and abnormal kinetics and voltage dependence. Conversely, LVA Ca^{2+} channels function normally without combining with other subunits [4].

All tetrameric ion channels share the main structural features, probably because they are likely to have evolved from common ancestor proteins, dating back to simple peptide ion channels. Moreover, phylogenetic analysis of ion channels seems to suggest that the Na_v channel evolved from an ancient Ca_v channel resembling the T-type channels [7,8]. Besides sharing structural features, tetrameric ion channels are characterized by a common distribution of charged residues over their corresponding molecular components. It will be shown that such a distribution facilitates the opening of tetrameric ion channels by way of a chain of attractive electrostatic interactions. This facilitated opening pathway starts from a channel conformation where the CP is closed on the intracellular side of the membrane and open on the extracellular side. This conformation immediately preceding channel opening is diametrically opposed to that proposed in a number of recent works, although it has found wide consensus in the early literature in connection with the opening of the squid axon Na^+ channel during the action potential.

2. The common structural features of tetrameric ion channels

The four S1–S4 helices of each domain form the so-called *voltage sensing domain* (VSD), with the S4 helix bearing 4 to 7 positive charges and the totality of the other three helices bearing a net negative charge.

https://doi.org/10.1016/j.elecom.2020.106866
Received 13 October 2020; Received in revised form 2 November 2020;
Available online 9 November 2020

The three S1–S3 helices of each VSD are arranged in such a way as to form a hydrophobic waist, ~10 Å in length, called a *gating pore*, interposed between two hydrophilic vestibules. By convention, the transmembrane potential ϕ measures the electric potential inside the cell relative to that outside. As ϕ is made sufficiently positive, the resulting electrostatic repulsion moves the four positively charged S4 helices outwards (i.e., toward the extracellular side of the membrane) in a stepwise fashion along their own gating pore. The total number of charges of the four S4 helices that pass across the corresponding gating pores following their outward movement constitutes the *gating charge*.

Fig. 2 shows two opposite domains, where each of the two VSDs is schematically represented by an hourglass showing only the S4 helix in outward position inside its own VSD, whose constriction simulates the gating pore.

In moving outward, each S4 helix rotates so as to form transient ion pairs with the negative charges located in the corresponding S1–S3 helices [1]. The four VSDs are located at the corners of a square, with the central pore (CP) at its center, floating as if they were separate from the CP. The upward movement of each S4 helix, induced by a positive potential step (the *depolarizing pulse*), is transmitted through a S4–S5 linker to the corresponding S5 helix, which makes many amino acid contacts with the corresponding S6 helix on the intracellular surface of the membrane. The four S6 helices, flanked by the relative S5 helices, are widely separated near the extracellular membrane surface, whereas they converge at the intracellular membrane surface, where they form a sort of bundle crossing, called an *activation gate*, which can be either open or closed.

On the extracellular side of the membrane, the four S5 helices are linked to the corresponding S6 helices by four extended loops (the *P loops*), which are partially folded back into the CP, lining its outer portion and forming a funnel-like vestibule, called a *selectivity filter* (SF). This name stems from the fact that the folded back loops contain a highly conserved amino acid sequence, called the *signature sequence*. The peptide chains of the signature sequence can replace the hydration shell of the permeant ion, allowing or inhibiting its flow. In view of its function, the SF is also called an inactivation gate and can be either open or inactive. The CP shows a swelling (cavity) at about half its full length and is filled with water. It is enclosed between the activation gate at the intracellular membrane surface and the SF at the extracellular one. The rapid closure of the activation gate is determined by its plugging up by a portion of some intracellular loop, referred to as the *endogenous blocker*, whose receptor is located inside the CP, below the SF.

The above features are common to all voltage-gated K^+, Na^+, and Ca^{2+} channels, which exploit them by moving the permeant ion from the membrane side, where its concentration is higher, to that where it is lower. For this reason, the K^+ ion, whose concentration is about two orders of magnitude higher on the intracellular side of the membrane, moves from this side to the extracellular side along the K^+ channel,

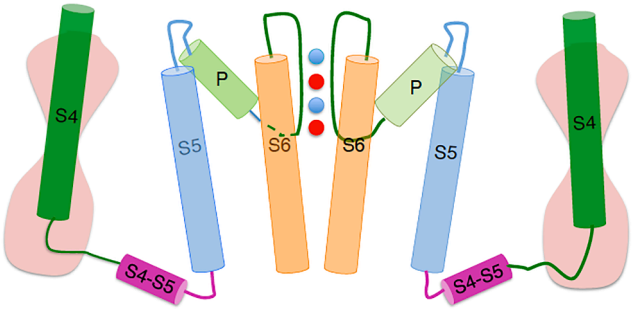

Fig. 2. Schematic picture of two opposite domains, simplified by removing the S1–S3 helices of each VSD and replacing them by an hourglass symbolizing two hydrophilic vestibules separated by the gating pore. The cylinders denote α-helices, whereas the curved lines connecting the cylinders denote intra- or extracellular loops.

generating a current that is conventionally positive. Conversely, Na^+ and Ca^{2+}, whose concentrations are decidedly higher on the extracellular side of the membrane, move from this side to the intracellular side along the corresponding ion channels, generating currents that are conventionally negative. More precisely, K^+ ions enter the water-filled CP of the K^+ channel through the activation gate, release their hydration shell to the SF and emerge in the extracellular aqueous solution while reconstituting their hydration shell. Na^+ and Ca^{2+} ions move along the corresponding channels following the opposite pathway.

3. Common charge distributions in the components of tetrameric ion channels

In addition to the above common structural features of all three tetrameric ion channels, other common features are significant in order to understand the important role played by electrostatic interactions in the structure–function relationship of these channels. Thus:

1. The sum of the charges of the S1, S2 and S3 helices participating in any VSD is negative.

   A single S1 helix carries one positive charge in the K_v1 K^+ channel, and no charges in the K_v2 and Shaker K^+ channels [9]. Incidentally, when a charge is exactly located at the border of a helix, a margin of arbitrariness exists in ascribing it to the helix or not. The S2 helix carries one net negative charge in K_v1, and two net negative charges in K_v2 and Shaker K^+ channel. Two of these negative charges, called glutamates E_0 and E_1, are on opposite sides with respect to the gating pore of each VSD, where the electric field of the whole VSD is focused. They are said to constitute a *charge transfer center* because they were found to facilitate the movement of gating charges across

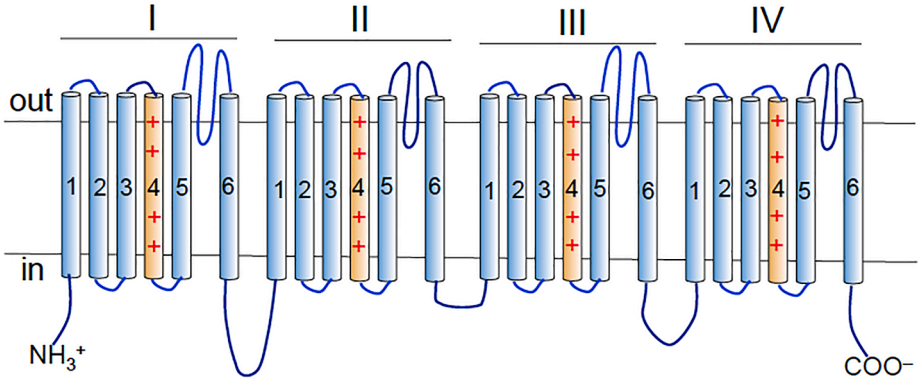

Fig. 1. Polypeptide chain of a Na^+ or Ca^{2+} channel. The four domains, from I to IV, consist of six transmembrane α-helices; cylinders denote α-helices, whereas the curved lines connecting the cylinders denote intra- or extracellular loops.

the gating pore [10]. This feature is believed to be common to all voltage-gated ion channels [11]. The S3 helix carries two negative charges in $K_v2.1$ and Shaker K^+ channel, and three in $K_v1.2$. The human Na^+ channel $Na_v1.7$DIV carries one net negative charge in S1, S2 and S3 [12]. In T-type Ca^{2+} channels, S1 and S2 have a zero net charge, whereas S3 has two net negative charges [4].

2. All S5–S6 loops, with their intermediate portion folded back into the upper portion of the CP to form the SF, are negatively charged.

   The charge contributed by the totality of the four domains to the sole SF equals –4*e* for Na^+ channels (except for the rat skeleton muscle Na^+ channel, where it equals –5*e*), –8*e* for Ca^{2+} channels, and 0 for Shaker and K_vAP K^+ channels [13]. With the exclusion of K^+ channels, the total charge of the SF is twice that of the two permeant ions usually considered to simultaneously reside in the SF, alternated with water molecules [14]. The SF charges being twice in magnitude but opposite in sign to those expected to be carried by two permeant ions simultaneously present in the SF has the effect of attracting neighboring cations toward the SF. In the case of the K^+ channel, the charge carried by the totality of the S5–S6 loops is sufficient to exert an attractive interaction upon K^+ ions, being –4*e* for $K_v2.1$, –16*e* for $K_v1.2$, and –8*e* for the Shaker K^+ channel [9]. The net negative charge carried by the S5–S6 loops of all four domains of the human brain HBA Na^+ channel amounts to ~–15*e* [15]. The totality of the four S5–S6 loops carry a net charge of ~–8*e* in Ca_v1, ~ –6*e* in Ca_v2 and ~–8*e* in Ca_v3 [16].
3. All endogenous blockers bear a net positive charge.

   It is generally accepted that the blocker of the Shaker K^+ channel consists of the 'ball-and-chain' motif present in any of the four N-termini of the K^+ channel subunits. The first amino acids of the N-terminus constitute the ball domain. This consists of 11 hydrophobic amino acids, 8 hydrophilic ones and 4 positively charged ones. The following 60 amino acids constitute the chain domain [17]. There is also general consensus that the CP of the Na^+ channel is blocked by the so-called 'hinged lid' motif, present in the III–IV loop and containing a hydrophobic triad of isoleucine, phenylalanine and methionine, briefly denoted by IFM [18]. The folded region enclosed between the two opposite hinges of the lid is positively charged, since it contains six lysine residues in the face of one aspartate and two glutamate residues [19]. Analogously, the intracellular I–II loop of HVA Ca^{2+} channels, which has been proposed as an important determinant of the voltage dependent inactivation phase [20], has a net positive charge [21]. A number of pieces of experimental evidence suggest that the positively charged intracellular III–IV loop is the most probable candidate for blocker of the Ca_v 3.1 Ca^{2+} channel [22]; at any rate, even all other intracellular loops of Ca_v3 Ca^{2+} channels bear a net positive charge [4].

A further feature that the three tetrameric ion channels share, albeit confined to channels containing one or more glutamate (E) residues in the SF, is the effect of E protonation/deprotonation in the proximity of physiological pH values. In this connection, it must be noted that the pK of ionizable groups buried inside the low dielectric environment of bulky proteins is quite different from that in water. In particular, the E residue assumes values around 7 [23]. Particularly rich in E residues are $Ca_v1.2$ Ca^{2+} channels and prokaryotic NaChBac, Na_vAB and Na_vRh Na^+ channels, which contain four E residues [13]. The Shaker K^+ channel contains no E residues in the SF, but a number of prokaryotic K^+ channels, including KcsA and the inward rectifier KIR family, contain four E residues in the SF. While wild-type KcsA yields a stable tetramer, its E71V mutant is mainly monomeric [24]. Moreover, the inward current of the wild-type KcsA, albeit not completely negligible, tends to a plateau, whereas E71V causes it to increase more than the outward current. A collapse of KcsA similar to the so-called C-type inactivation was shown not to occur with the E71A mutant [25].

The effect of external protons on single Na^+ channel currents recorded on guinea pig ventricular myocytes was first reported by Zhang and Siegelbaum in 1991 [26]. Many simulations dealing with this pH effect have recently been carried out on prokaryotic Na^+ channels (see [27] and references therein), because their structures are more clearly known (see, e.g., [28]) and simulations are less time consuming. It is often assumed that at physiological pH both the fully deprotonated and the singly and doubly protonated states of the SF are feasible. A simulation reported in [29] predicts a decrease in the average number of Na^+ ions in the SF from 2.3 to 2 as the E residues in the signature ring pass from fully deprotonated to singly protonated. This conclusion is quite intuitive, since a decrease in the negative charge in the SF causes a decrease the electrostatic attraction towards the positively charged Na^+ ions.

Eukaryotic L-type Ca^{2+} channels are pH dependent. Thus, an increase in proton concentration strongly inhibits ion permeation through open Ca^{2+} channels, while reducing channel opening. Using a combination of site-directed mutagenesis and single channel recording of wild-type and mutated L-type Ca^{2+} channels, direct evidence was provided that protons block the Ca^{2+} channel by interacting with a site located along the permeation pathway [30]. More precisely, the protonation site was identified in a specific subset of E residues within the P-loop.

4. The sequence of conformational states during ion channel opening

The activation gate can be either open (O) or closed (C), whereas the SF can be either open (O) or inactivated (I). The different conformations of the ion channels will be denoted by first specifying the state of the activation gate and then the state of the SF (i.e., the inactivation gate), and by separating the symbols of the two states with a slash. A particularly significant conformational state is that which immediately precedes the open state (O/O), where both activation and inactivation states are open. Practically all recent papers identify this state with (O/I). This is the case with the so-called 'open state sequence' proposed by Bähring and Covarrubias for Na^+ channels and, putatively, for Ca^{2+} ones [31]. An analogous direct passage from (O/I) to (O/O) was also proposed by Hering for the HVA $Ca_v1.2$ Ca^{2+} channel [32] and by Jensen et al. for the K^+ channel [33].

A diametrically opposed (C/O) conformation immediately preceding ion channel opening was proposed in the early literature for the squid axon Na^+ channel during the action potential [34]. This conformation satisfies the intuitive expectation of a depolarizing pulse moving outward the S4 helix, which is initially inward in accordance with a closed activation gate. This conformation was also included by us in the sequences for Shaker K^+ [35] and $Ca_v3.1$ Ca^{2+} channels [22].

It is the direct passage from the (C/O) to the (O/O) conformation that takes full advantage of favorable attractive electrostatic interactions. Thus, the stepwise upward movement of the four S4 helices following a depolarizing pulse leaves behind an increasing negative charge in the lower vestibule of their VSDs; this exerts a progressively stronger attractive interaction on the positively charged blocker, until the latter completely plugs the CP and extinguishes the ionic current. A further electrostatic contribution to the CP obstruction by the positively charged blocker comes from the negative charges on the extracellular side with respect to the receptor, such as the net negative charge in the extracellular S5–S6 loops surrounding the funnel-like vestibule of the SF.

The assumption of a stepwise outward movement of the S4 helices as a consequence of a depolarizing pulse is required to account for the salient features of tetrameric ion channels by the use of only two, or at most three, free parameters [19,22,35,36]. Support for this assumption comes from the analysis of the noise of the gating currents of a high number of Na^+ [37] and Shaker K^+ [38] channels, which is consistent with the occurrence of gating charge movements by at least 2.4 *e* steps. This fractional charge is slightly less than one fourth of the total gating charge moved by a Na^+ [39] or Shaker K^+ channel [40], suggesting that it is associated with the movement of a single domain of these ion channels. It is quite natural to infer that this stepwise gating charge

movement is associated with the stepwise movement of the S4 helices of Na^+ and Shaker K^+ channels.

In conclusion, the common structural features and charge distribution of tetrameric voltage-gated ion channels point to an energetically favored pathway of channel opening. This pathway starts from a conformation with the activation gate closed and the inactivation gate open. Following a depolarizing pulse, the stepwise outward movement of the four S4 helices triggers a series of interlinked electrostatic attractive interactions that lead to complete opening of the ion channels.

CRediT authorship contribution statement

Rolando Guidelli: Conceptualization, Methodology, Data curation, Writing - original draft, Writing - review & editing.

Declaration of Competing Interest

The author declares that he has no known competing financial interests or personal relationships that could have appeared to influence the work reported in this paper.

Appendix

Stochastic kinetic models of tetrameric ion channels

The above conclusions are based on a deterministic approach to the kinetic treatment of tetrameric ion channels [19,22,35,36]. Such an approach results in exact outputs for a fixed set of initial conditions, no matter how many times the model reruns the calculations. The low number of free parameters (two, or at most three) allows a precise physical meaning to be attached to all of them. Practically all other kinetic models of tetrameric ion channels are Markov stochastic models, which assume that future states depend only on the present state, and not on the events that preceded it. The probability of being in a state S_i represents the fraction of channels in state S_i, and the transition probabilities from state S_i to state S_j become the rate constants of the forward and backward reactions between S_i and S_j. The fact that the same set of parameter values and initial conditions leads to an ensemble of different outputs imparts to stochastic models an inherent flexibility, allowing them to interpret a great number of experimental features, albeit by the use of a relatively high number of free parameters. This may cause a lack of structural identifiability, arising from the fact that two or more distinct underlying processes can yield clustered processes with identical probabilistic properties [41]. Moreover, a high number of free parameters do not allow a precise physical significance to be attached to them.

Since the existence of ion channels was confirmed, several activation schemes of progressively increasing complexity have been proposed, especially with K^+ channels, and almost all of them have maintained one feature of the Hodgkin–Huxley model, namely their ending in a single final open state. Many of these models account for the structure of tetrameric ion channels by including four parallel pathways of activation [42]. Once all four subunits reach a permissive state, the pathways merge and the channel experiences additional series of concerted transitions, some of which may involve stepwise movement of charge [43], before opening. All these models have little in common with each other, with different models explaining the same experimental data through very different mechanisms. Some stochastic models adopt an allosteric mechanism where horizontal steps between different closed states are combined with vertical steps leading to different open states [44,45]. A stochastic model that applies to all tetrameric channels was developed in [46]. In this model, each subunit (or domain) undergoes several conformational changes during channel gating, independent of the state of the other subunits, before reaching a permissive state. Transition from the permissive state of all four subunits to the open state involves their concerted movement. A simplified approach was developed to incorporate the cooperative transition directly from the subunit models. Experimental data were nicely fitted by this model through a 16×16 transition rate matrix requiring 16 free parameters.

References

[1] W.A. Catterall, Structure and function of voltage-gated sodium channels at atomic resolution, Exp. Physiol. 99 (2014), https://doi.org/10.1113/expphysiol.2013.071969.

[2] A.L. Goldin, T. Snutch, H. Lubbert, A. Dowsett, J. Marshall, V. Auld, W. Downey, L. C. Fritz, H.A. Lester, R. Dunn, Messenger RNA coding for only the alpha subunit of the rat brain Na channel is sufficient for expression of functional channels in Xenopus oocytes. Proc. Natl. Acad. Sci. 83 (19) (1986) 7503–7507, https://doi.org/10.1073/pnas.83.19.7503.

[3] B. Simms, G. Zamponi, Neuronal voltage-gated calcium channels: structure, function, and dysfunction, Neuron 82 (1) (2014) 24–45, https://doi.org/10.1016/j.neuron.2014.03.016.

[4] E. Perez-Reyes, Molecular physiology of low-voltage-activated T-type calcium channels, Physiol. Rev. 83 (1) (2003) 117–161, https://doi.org/10.1152/physrev.00018.2002.

[5] J. Wu, Z. Yan, Z. Li, X. Qian, S. Lu, M. Dong, Q. Zhou, N. Yan, Structure of the voltage-gated $Ca_v1.1$ at 3.6 Å resolution, Nature 537 (2016) 191–196, https://doi.org/10.1038/nature19321.

[6] Y. Zhao, G. Huang, Q. Wu, K. Wu, R. Li, J. Lei, X. Pan, N. Yan, Cryo-EM structures of apo and antagonist-bound human $Ca_v3.1$, Nature 576 (7787) (2019) 492–497, https://doi.org/10.1038/s41586-019-1801-3.

[7] J.D. Spafford, A.N. Spencer, W.J. Gallin, Genomic organization of a voltage-gated Na^+ channel in a hydrozoan jellyfish: insights into the evolution of voltage-gated Na^+ channel genes, Recept. Chan. 6 (1999) 493–506.

[8] B.J. Liebeskind, D.M. Hillis, H.H. Zakon, Evolution of sodium channels predates the origin of nervous systems in animals, Proc. Natl. Acad. Sci. 108 (22) (2011) 9154–9159, https://doi.org/10.1073/pnas.1106363108.

[9] S.B. Long, X. Tao, E.B. Campbell, R. MacKinnon, Atomic structure of a voltage-dependent K^+ channel in a lipid membrane-like environment, Nature 450 (7168) (2007) 376–382, https://doi.org/10.1038/nature06265.

[10] X. Tao, A. Lee, W. Limapichat, D.A. Dougherty, R. MacKinnon, A Gating Charge Transfer Center in Voltage Sensors, Science 328 (5974) (2010) 67–73, https://doi.org/10.1126/science:1185954.

[11] C.M. Armstrong, S. Hollingworth, A perspective on Na and K channel inactivation, J. Gen. Physiol. 150 (2018) 7–18, https://doi.org/10.1085/jgp.201711835.

[12] A. Sula, J. Booker, L.C.T. Ng, C.E. Naylor, P.G. DeCaen, B.A. Wallace, The complete structure of an activated open sodium channel, Nature Commun. 8 (2017) 14205. https://www.nature.com/articles/ncomms14205.

[13] R.K. Finol-Urdaneta, Y. Wang, A. Al-Sabi, C. Zhao, S.Y. Noskov, R.J. French, Sodium channel selectivity and conduction: prokaryotes have devised their own molecular strategy, J. Gen. Physiol. 143 (2014) 157–171, https://doi.org/10.1085/jgp.201311037.

[14] Y. Zhou, J.H. Morais-Cabral, A. Kaufman, R. MacKinnon, Chemistry of ion coordination and hydration revealed by a K^+ channel-Fab complex at 2.0 Å resolution, Nature 414 (2001) 43–48, https://doi.org/10.1038/35102009.

[15] C.M. Ahmed, D.H. Ware, S.C. Lee, C.D. Patten, A.V. Ferrer-Montiel, A.F. Schinder, J.D. McPherson, C.B. Wagner-McPherson, J.J. Wasmuth, G.A. Evans, Primary structure, chromosomal localization, and functional expression of a voltage-gated sodium channel from human brain. Proc. Natl. Acad. Sci. 89 (17) (1992) 8220–8224, https://doi.org/10.1073/pnas.89.17.8220.

[16] J.R. Tyson, T.P. Snutch, Molecular nature of voltage-gated calcium channels: structure and species comparison, WIREs Membr Transp Signal 2 (5) (2013) 181–206, https://doi.org/10.1002/wmts.91.

[17] Z.W. Hall, An Introduction to Molecular Neurobiology, 1st ed., Sinauer Associates, Sunderland, Mass, 1992, p. 113.

[18] W.A. Catterall, From ionic currents to molecular mechanisms, Neuron 26 (1) (2000) 13–25, https://doi.org/10.1016/S0896-6273(00)81133-2.

[19] R. Guidelli, L. Becucci, Modeling squid axon Na^+ channel by a nucleation and growth kinetic mechanism, Biochimica et Biophysica Acta (BBA) - Biomembranes 1861 (1) (2019) 100–109, https://doi.org/10.1016/j.bbamem.2018.08.009.

[20] S.C. Stotz, S.E. Jarvis, G.W. Zamponi, Functional roles of cytoplasmic loops and pore lining transmembrane helices in the voltage-dependent inactivation of HVA calcium channels, J. Physiol. 554 (2004) 263–273, https://doi.org/10.1113/jphysiol.2003.047068.

[21] T.V. Starr, W. Prystay, T.P. Snutch, Primary structure of a calcium channel that is highly expressed in the rat cerebellum. Proc. Natl. Acad. Sci. 88 (13) (1991) 5621–5625, https://doi.org/10.1073/pnas.88.13.5621.

[22] R. Guidelli, L. Becucci, Deterministic model of $Ca_v3.1$ Ca^{2+} channel and a proposed sequence of its conformations, Bioelectrochemistry 136 (2020) 107618, https://doi.org/10.1016/j.bioelechem.2020.107618.

[23] M.J. Harms, C.A. Castañeda, J.L. Schlessman, G.R. Sue, D.G. Isom, B.R. Cannon, B. García-Moreno E., The pK_a values of acidic and basic residues buried at the same internal location in a protein are governed by different factors, J. Mol. Biol. 389 (1) (2009) 34–47, https://doi.org/10.1016/j.jmb.2009.03.039.

[24] HoSook Choi, L. Heginbotham, Functional influence of the pore helix glutamate in the KcsA K^+ channel, Biophys. J. 86 (4) (2004) 2137–2144, https://doi.org/10.1016/S0006-3495(04)74273-3.

[25] M.P. Bhate, A.E. McDermott, Protonation state of E71 in KcsA and its role for channel collapse and inactivation, Proc. Natl. Acad. Sci. USA 109 (38) (2012) 15265–15270, https://doi.org/10.1073/pnas.1211900109.
[26] J.-F. Zhang, S.A. Siegelbaum, Effects of external protons on single cardiac sodium channels from guinea pig ventricular myocytes, J. Gen. Physiol. 98 (1991) 1065–1083.
[27] A. Damjanovic, A.Y. Chen, R.L. Rosenberg, D.R. Roe, X. Wu, B.R. Brooks, Protonation state of the selectivity filter of bacterial voltage-gated sodium channels is modulated by ions, Proteins 88 (3) (2020) 527–539, https://doi.org/10.1002/prot.25831.
[28] M.J. Lenaeus, T.M. Gamal El-Din, C. Ing, K. Ramanadane, R. Pomès, N. Zheng, W. A. Catterall, Structures of closed and open states of a voltage-gated sodium channel, Proc. Natl. Acad. Sci. USA 114 (15) (2017) E3051–E3060, https://doi.org/10.1073/pnas.1700761114.
[29] C. Boiteux, I. Vorobyov, T.W. Allen, Ion conduction and conformational flexibility of a bacterial voltage-gated sodium channel, Proc. Natl. Acad. Sci. 111 (9) (2014) 3454–3459, https://doi.org/10.1073/pnas.1320907111.
[30] X.-H. Chen, I. Bezprozvanny, R.W. Tsien, Molecular basis of proton block of L-type Ca^{2+} channels, J. Gen. Physiol. 108 (1996) 363–374, https://doi.org/10.1085/jgp.108.5.363.
[31] R. Bähring, M. Covarrubias, Mechanisms of closed-state inactivation in voltage-gated ion channels, J. Physiol. 589 (2011) 461–479, https://doi.org/10.1113/jphysiol.2010.191965.
[32] S. Hering, E.-M. Zangerl-Plessl, S. Beyl, A. Hohaus, S. Andranovits, E.N. Timin, Calcium channel gating, Pflügers Archiv – Eur. J. Physiol. 470 (2018) 1291–1309, https://doi.org/10.1007/s00424-018-2163-7.
[33] M.O. Jensen, V. Jogini, D.W. Borhani, A.E. Leffler, R.O. Dror, D.E. Shaw, Mechanism of voltage gating in potassium channels, Science 336 (6078) (2012) 229–233, https://doi.org/10.1126/science:1216533.
[34] F.H. Martini, Anatomy and Physiology, Chapter 12. The Nervous System and Nervous Tissue, Pearson Education Inc., S. Francisco, 2007.
[35] R. Guidelli, L. Becucci, Merging *Shaker* $^{K}+$ channel electrophysiology with structural data by a nucleation and growth mechanism, Electrochim. Acta 301 (2019) 390–400, https://doi.org/10.1016/j.electacta.2019.01.183.
[36] R. Guidelli, L. Becucci, Modeling squid axon K^+ channel by a nucleation and growth kinetic mechanism, Biochimica et Biophysica Acta (BBA) - Biomembranes 1860 (2) (2018) 505–514, https://doi.org/10.1016/j.bbamem.2017.11.009.
[37] F. Conti, W. Stuhmer, Quanta charge redistributions accompanying the structural transitions of sodium channels, Eur. Biophys. J. 17 (1989) 53–59, https://doi.org/10.1007/BF00257102.
[38] D. Sigg, E. Stefani, F. Bezanilla, Gating current noise produced by elementary transitions in *Shaker* potassium channels, Science 264 (5158) (1994) 578–582, https://doi.org/10.1126/science:8160016.
[39] B. Hirschberg, A. Rovner, M. Lieberman, J. Patlak, Transfer of twelve charges is needed to open skeletal muscle Na^+ channels, J. Gen. Physiol. 106 (1995) 1053–1068, https://doi.org/10.1085/jgp.106.6.1053.
[40] N. Schoppa, K. McCormack, M. Tanouye, F. Sigworth, The size of gating charge in wild-type and mutant *Shaker* potassium channels, Science 255 (5052) (1992) 1712–1715, https://doi.org/10.1126/science:1553560.
[41] F.G. Ball, J.A. Rice, Stochastic models for ion channels: Introduction and bibliography, Math. Biosci. 112 (2) (1992) 189–206, https://doi.org/10.1016/0025-5564(92)90023-P.
[42] D. Sigg, F. Bezanilla, A physical model of potassium channel activation: from energy landscape to gating kinetics, Biophys. J . 84 (6) (2003) 3703–3716, https://doi.org/10.1016/S0006-3495(03)75099-1.
[43] N.E. Schoppa, F.J. Sigworth, Activation of Shaker potassium channels. I. Characterization of voltage-dependent transitions, J. Gen. Physiol. 111 (1998) 271–294, https://doi.org/10.1085/jgp.111.2.271.
[44] C. Gonzalez, H.P. Koch, B.M. Drum, H.P. Larsson, Strong cooperativity between subunits in voltage-gated proton currents, Nat. Struct. Mol. Biol. 17 (2010) 51–56. https://www.nature.com/articles/nsmb.1739.
[45] S.M.E. Smith, T.E. DeCoursey, Consequences of dimerization of the voltage gated proton channel, 117 (2013) 335–360, in: J.Giraldo, F. Ciruela (Eds.), Progress in Molecular Biology and Translational Science; Oligomerization in Health and Desease, Chapter 12. Academic Press, Cambridge, MA 02139, U.S.A. https://doi.org/10.1016/B978-0-12-386931-9.00012-X.
[46] A. Nekouzadeh, J.R. Silva, Y. Rudy, Modeling subunit cooperativity in opening of tetrameric ion channels, Biophys. J. 95 (7) (2008) 3510–3520, https://doi.org/10.1529/biophysj.108.136721.